Wavelet Analysis, New Signal Processing Method, Used for Detection a Broken Rotor Bars in AC Motor

ELEONORA DARIE
Electrotechnical Department
Technical University of Civil Engineering
B-dul Pache Protopopescu 66, Sector 2, Bucharest
ROMANIA
eleonora_darie@yahoo.com

EMANUEL DARIE
Engineering Department
Police Academy
Aleea Privighetorilor 1A, Sector 1, Bucharest
ROMANIA
edarie@yahoo.com

Abstract: - This work describes a useful method for detection broken rotor bars in AC motors. The start-up transient current of an induction machine is used as the medium for diagnoses. The fundamental component is extracted using an algorithm that predicts the instantaneous amplitude and frequency during start-up. The residual current is then analyzed using wavelets and a comparison is made between a healthy and damaged machine. This method of machine condition monitoring is not load dependant and can be used for machines that are unloaded.

Key-Words: - AC Motor, Electrical Diagnostics, Fast Fourier Transform, Signal Processing, Spectral Analysis, Wavelet Transform.

1 Introduction

Induction motors are inherently reliable and require minimum maintenance. However, like other motors, they eventually deteriorate and fail. This gives rise to the need for cost effective preventive maintenance based on condition monitoring, which can be addressed by monitoring and analyzing the real-time signals of the motors.

The broken rotor bar fault at an early stage or partially broken rotor bars, which can lead to a larger failure or even be catastrophic, may not be detectable even under full load conditions. Therefore, mere is a strong need to develop condition monitoring techniques to address mess issues to allow earlier detection of rotor faults.

Broken rotor bars can be a serious problem with certain induction motors due arduous cycles. Although broken rotor bars do not initially cause a motor to fail, there can be serious secondary effects. The fault mechanism can result in broken parts of the bar hitting the end winding or stator core of a high voltage motor at a high velocity.

The most part of the methods of induction machine monitoring utilize the steady-state spectral components of the stator. These spectral components include voltage, current and power and are used to detect broken rotor bars, bearing failures and air gap eccentricity.

Broken rotor bars [3, 4] are one of the easiest AC Motor faults to detect using steady-state stator current condition monitoring. This is based on monitoring the amplitudes of the double slip frequency sidebands of the fundamental supply frequency in the current spectrum [1].

Due to the nature of the signal, the conventional Fast Fourier Transform analysis is not suitable for analyzing starting currents [2].

2 Problem Formulation

The broken rotor bars can be detected by monitoring the current spectral components [1]. These spectral components are illustrated by the following equation:

$$f_{brb} = f_s\left[\frac{k}{p}(1-s) \pm s\right], \quad (1)$$

where: f_s, p and s are, respectively, the electrical supply frequency, number of pole pairs and the per-unit split; k/p=1,5,7,11,13 ... due to the normal winding configuration. For k/p=1, the additional component in the current spectrum is (l-2s) f_s due to the broken rotor bar and (l+2s) f_s, owing to the speed oscillations.

From (1) it is evident that the rotor bar frequencies are a function of the machine slip. If the machine is unloaded, the slip will be almost zero. The rotor bar frequencies will be masked by the fundamental frequency and thus make detection difficult. The only solution is therefore to heavily load the machine in order to separate the frequencies. Overloading a machine is undesirable since it reduces the machine's operating lifetime and is not generally under control of the operator. Accurate detection therefore is difficult at light loading conditions. A fundamental disadvantage of the assumption of steady-state speed in condition monitoring is that there are many applications where constant speed operation is not achieved for example in wind generation or motor operated valves.

The frequencies form the stator current spectrum shown in Figure 1 and are present irrespective of the machine's condition.

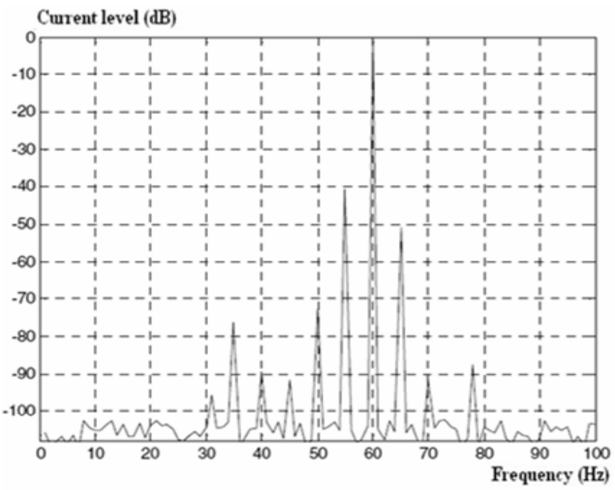

Fig. 1. The current spectrum of an AC Motor with broken rotor bars.

The presence of broken rotor bars is indicated by the difference in amplitude between the fundamental and the left sideband. A difference less than 50 dB is an indication of broken rotor bars [3-7]. The amplitude of the left sideband frequency component of the fundamental frequency is proportional to the number of broken rotor bars present [8].

3 Problem Solution

Wavelet Analysis is introduced as a tool for analyzing signals with frequency spectrum varying in time. It allows a time-localization of the frequency components occurring within the signal, being able to extract their time evolution. This property makes possible the detection of characteristic patterns within the evolution of those components, which can be related to the occurrence of certain phenomena.

Fourier analysis uses the basic functions sin (t), cos(t) and exp(it). In the frequency domain, these functions are perfectly localized, but they are not localized in the time domain, resulting in a difficult to analyze or synthesize complex signals presenting fast local variations such as transients or abrupt changes. To overcome the difficulties involved, it is possible to window the signal using a regular function which is zero or nearly zero outside a time segment.

The orthogonal basis functions used in Wavelet analysis are families of scaling functions, $\Phi(t)$, and associated wavelets, $\upsilon(t)$. The scaling function, $\Phi(t)$, can be represented by the following mathematical expression:

$$\Phi_{j,k}(t) = \sum_k H_k \Phi\left(2^j t - k\right), \tag{2}$$

where: H_k represents the coefficients of the scaling function, k is a translation and j represents the scale.

Similarly, the associated wavelet $\upsilon(t)$, can be generated using the same coefficients as the scaling function.

$$\upsilon_{j,k}(t) = \sum_k (-1)^k \sqrt{2}\, h_{1-k} \Phi\left(2^j t - k\right), \tag{3}$$

The scaling functions are orthogonal to each other as well as with the wavelet functions as shown in (3), (4). This fact is crucial and forms part of the framework for multi resolution analysis.

$$\int_{-\infty}^{+\infty} \Phi(2t-k) \cdot \Phi(2t-l) \mathrm{d}t = 0, \text{for all } k \neq l\,, \tag{4}$$

$$\int_{-\infty}^{+\infty} \upsilon(t) \cdot \Phi(t)\, \mathrm{d}t = 0 \,\cdot \tag{5}$$

Using an iterative method, the scaling function and associated wavelet can be computed if the coefficients are known.

A signal can be decomposed into approximate coefficients, $a_{j.k}$, through the inner product of the original signal at scale j and the scaling function.

$$a_{j,k} = \int_{-\infty}^{+\infty} f_j(t) \cdot \Phi_{j,k}(t)\, \mathrm{d}t\,, \tag{6}$$

$$\phi_{j,k}(t) = 2^{-j/2} \Phi\left(2^{-j} t - k\right). \tag{7}$$

Similarly the detail coefficients, $d_{j,k}$ can be obtained through the inner product of the signal and the complex conjugate of the wavelet function.

$$d_{j,k} = \int_{-\infty}^{+\infty} f_j(t) \cdot \upsilon^*_{j,k}(t)\, \mathrm{d}t\,, \tag{8}$$

$$\upsilon_{j,k}(t) = 2^{-j/2} \upsilon\left(2^{-j} t - k\right). \tag{9}$$

The original signal can therefore be reconstructed by a single series of scaling coefficients and a double series of the detail coefficients.

$$f(t) = \sum_{j=-\infty}^{\infty} a_{j_0,k} \cdot \Phi_{j_0,k} + \sum_{j=-\infty}^{j_0} \sum_{k=-\infty}^{\infty} d_{j,k} \cdot \upsilon_{j,k}(t)\,, \tag{10}$$

A discretized signal can be decomposed at different scales as follows:

$$f[n] = \sum_{k=0}^{N-1} a_{j,k} \cdot \Phi_{j,k}(t) = = \sum_{k=0}^{N-1} a_{j+1,k} \cdot \Phi_{j+1,k}(t) + \sum_{k=0}^{N-1} d_{j+1,k} \cdot \Gamma_{j+1,k}(t) \quad (11)$$

3.1 Algorithm for extracting the fundamental component of current

Let $u(t)$ denotes a signal comprising a sinusoidal component in addition to a number of additional components and noise. A sinusoidal component of this function $y(t) = A\sin(\omega t + \delta)$ is of interest where A is the amplitude, ω is the frequency, δ is the phase and $\phi(t) = \omega t + \delta$, represents the total phase of this component. Ideally, parameters A, ω and δ are fixed quantities; but in practice, this assumption does not hold true [4].

Let M be a continuous manifold containing all sinusoidal signals defined as:

$$M = \begin{cases} y(t,\theta),\ \theta_i \in R, \\ \theta_i \in \left[\theta^i_{\min}, \theta^i_{\max}\right], i = 1,\ldots,n, y : Sinusoid \end{cases} \}$$

where is the vector of parameters which belongs to the parameter space

$\Theta = \{[\theta_1(t),\ldots,\theta_n(t)]^T \theta_i \in \left[\theta^i_{\min}, \theta^i_{\max}\right], i = 1,\ldots,n\}$,

and superscript T denotes matrix transposition. The objective is to find an element in M which is closest to the sinusoidal component of the signal $u(t)$. The solution has to be an orthogonal projection of $u(t)$ onto manifold M, or equivalently it has to be an optimum θ which minimizes a distance function d between $y(t;\omega(t))$ and $u(t)$, $\theta_{opt} = \arg\min_{\theta(t)\in\Theta} d[y(t,\theta(t),u(t)]$ [4].

The following instantaneous distance function d is used:

$$d(t,\theta(t)) = [u(t) - y(t,\phi(t))] = \mathrm{e}(t). \quad (12)$$

Hence, the cost function is defined as $J(t,\theta(t)) = \mathrm{d}^2(t,\theta(t))$. Although the cost function is not necessarily quadratic, the parameter vector θ is estimated using the gradient descent method.

$$\frac{d\theta(t)}{dt} = -\mu \frac{\partial J(t,\theta(t))}{\partial\theta(t)}. \quad (13)$$

The algorithm employing this method converges to the minimum solution for the cost function.

The output signal is defined as:

$$y(t) = A(t)\sin\left[\int^t \omega(\tau)d\tau + \delta(t)\right]. \quad (14)$$

Formulating the algorithm accordingly using the parameter vector $\theta = [A,\delta,\omega]$, the amplitude, phase angle and frequency of the desired component, results in the following set of equations:

$$\dot{A}(t) = \mu_1\, e(t)\sin\,\Phi(t)\,, \quad (15)$$

$$\dot{\omega}(t) = \mu_2\, A(t)\cos\,\Phi(t)\,, \quad (16)$$

$$\dot{\theta}(t) = \mu_1\mu_2\, e(t)A(t)\cos\theta(t) + \omega(t)\,, \quad (17)$$

$$y(t) = A(t)\sin\phi(t)\,, \quad (18)$$

$$e(t) = u(t) - y(t)\,. \quad (19)$$

In the equations (15) to (19), the time variable t is replaced by a constant number. This replacement converts the time-varying system into a time-invariant system. The apparently arbitrary formulation of the algorithm calls for mathematically justification which is presented here. The dot on top (·) represents the differentiation with respect to time. Note, that $\dot{\phi} = \xi + \dot{\delta}$, is used in deriving the third differential equation. State variables $A(t)$, $\theta(t)$ and $\omega(t)$ directly provide instantaneous estimates of the amplitude, phase and frequency of the extracted sinusoid, respectively. Undesired components and noise imposed on the sinusoidal component of interest altogether are provided by $e(t)$. The parameters μ_1, μ_2 and μ_3 are positive numbers which determine the behavior of the algorithm in terms of convergence rate versus accuracy.

Equations (15) to (19) constitute the governing set of equations of the generalized algorithm [4] used of extracting a specified sinusoidal signal, estimating its amplitude, frequency and phase, and accommodating variations in the amplitude, frequency and phase of such a sinusoidal component.

3.2 Numerical analysis

Two identical rotors (P_n = 750 W) induction motor are used in numerical analysis except that one had a broken rotor bar.

The same bearings and stator was used in order to minimize their influences on the start-up transients. The machine was analyzed under loading conditions varying from 30 % to 100 % to determine if this method of detection could be successful and independent of the loading conditions.

The start-up current transients of a 750 W induction motor are shown in Figure 2. Before implementing the fundamental extraction algorithm, the individual current is transformed into a single rotating current vector.

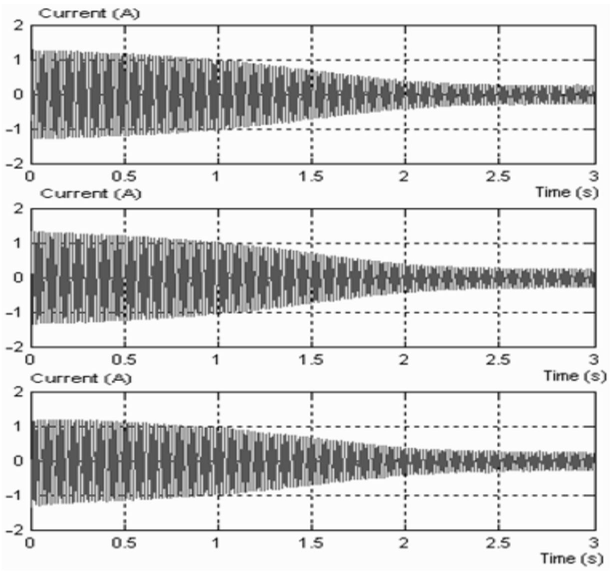

Fig. 2. Start up current transients for phases A, B and C.

It was found that the motor had a very low inertia and detection could not be done below 30 % loading because the transient times were too short. This vector is then transformed into the time domain and used as an input to the extraction algorithm.

The fundamental component is extracted with this algorithm. The resulting waveform shown in Figure 3 has information relating to the health of the machine including bad bearings, broken rotor bars etc.

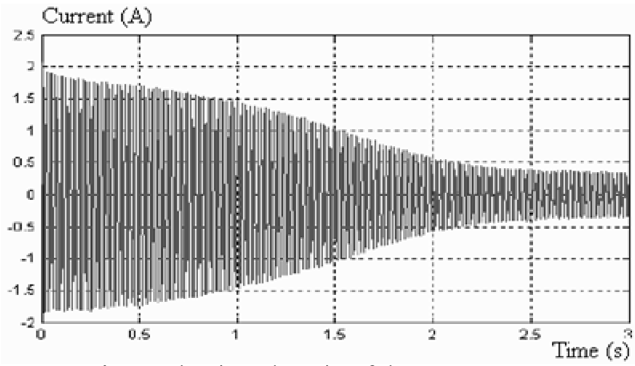

Fig. 3. The time domain of the current vector.

This vector is then transformed into the time domain and used as an input to the extraction algorithm. The fundamental component is extracted with this algorithm.

The resulting waveform shown in Figure 3 has information relating to the health of the machine including bad bearings, broken rotor bars etc.

The methodology employed was to apply the discrete wavelet transform to the residual current. The family of Daubechies wavelets was chosen as the basis functions for the decomposition. The family of Daubechies wavelets is classified according to the number of vanishings moments, N [4]. The smoothness of the wavelets increases with the number of vanishing moments.

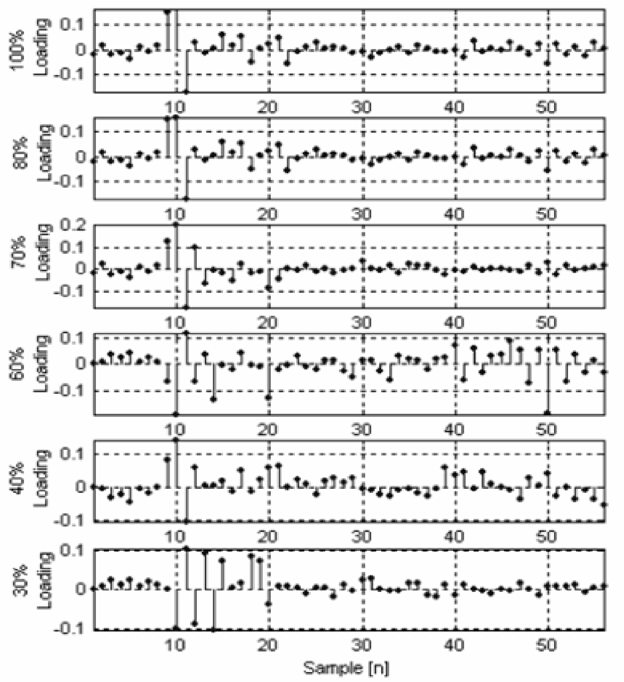

Fig. 4. Wavelet decomposition levels D9 of a healthy machine loaded 30 % to 100%.

For the case when N=1, the Daubechies scaling function are discontinuous. It is desirable to have smooth wavelets and therefore N is increased. Although the Dubechies2 wavelet is continuous, its derivatives are discontinuous. For N>2, the wavelet and its derivative are both continuous. It has shown in applications such as compression, noise removal and singularity detection, that the number of vanishing moments plays a key role for efficient coding of signals.

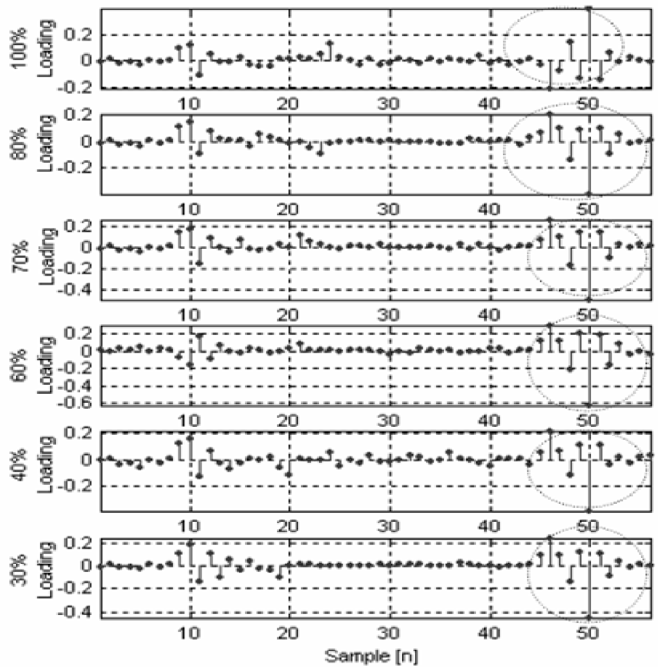

Fig. 5. Wavelet decomposition levels D9 of a damaged machine loaded 30 % to 100%.

The fundamental frequency of the stator current vector was removed from the total current using the extraction algorithm. The discrete wavelet transforms Daubechies8 wavelet, on applied to the residual current vector.

Figures 4 and 5 indicate the level 9 coefficients of both healthy and damaged machine under various loads. By inspection of figures 4 and 5, two dominant features are present that characterize the condition of the machine. The first feature is found between samples 8 and 13 of all the loading conditions. The feature is present in both the healthy and damaged machine. The second feature found between samples 45 and 53 is only present in the case of the damaged machine. An automated fault detection analyzer is envisioned based on this algorithm. The algorithm takes a few cycles to converge to the amplitude and frequency of the fundamental. This is shown in Figure 6.

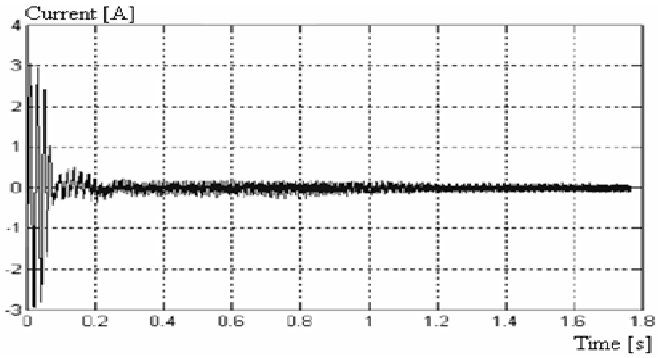

Fig. 6. The start up current after extraction of the fundamental.

As a result when the estimated fundamental is subtracted from the original waveform, the algorithm's output between 0 and 0.4 seconds should be discarded to allow for convergence. Figure 6 shows the estimated frequency of the fundamental. An accurate estimate of the frequency is only available after 0.4s.

4 Conclusion

This work investigates the detection of broken rotor bars using wavelet analysis of the starting current. The wavelet technique presented is able to extract useful characteristics of a transient signal, such as the starting current of an induction motor, and distinguish healthy and faulty motors by means of a numerical value called the wavelet indicator.

The wavelet indicator can also be used to classify the different degrees of broken rotor bar faults. As a general rule, the higher the value of the wavelet indicator is, the greater the severity of the fault.

Although the results of the partial broken rotor bars do not provide a clear indication about the severity of the fault, miss is primarily due to the small size of the motor under test. Due to miss, the effect of the resistance change under partial broken rotor bar is minimal. The broken rotor bars can be detected by the decomposition of the start-up current transient. This method has advantages over the traditional steady-state condition monitoring methods. It is not load dependant and can be effective on small lightly loaded machines. The machine does not have to be heavily loaded to make an accurate assessment of the machine's condition. There is no need for speed, torque or vibration measurement [9]. The analysis clearly shows that that the broken rotor bar can be detected using transient results only. This method can be used for standard induction motors, but also for machines that operate predominantly in the transient like wind generators or motor operated valves.

References:

[1] Eleonora Darie, A Wavelet Analysis model for detection of broken rotor bars in Induction Machines, *Proc. of 4 th International Conference: Metrology & Measurement Systems - METSIM 2007,* University Politehnica of Bucharest, Faculty of Electrical Engineering, Bucharest, ISSN 1843-648X, 2007.

[2]. A. Bellini, G. Franceschini, Quantitative evaluation of induction motor broken bars by means of electrical signature analysis, *Proc. IEEE. Trans. Indust. Electronics*, Vol. 37, No. 2, 2003, pp. 1248-1245.

[3] T. J. E. Miller, A Review of Induction Motors Signature Analysis as a Medium for Faults Detection, *Proc. IEEE. Trans. Indust. Electronics*, Vol. 47, No. 4, 2002, pp. 463-464.

[4] I. Daubechies, The wavelet transform time-frequency localization and signal analysis, *Proc. IEEE Trans. Indust. Electron.* Vol. 36, No. 3, 2001, pp. 961-1005.

[5] A. A. Da Silva, Rotating machinery monitoring and diagnosis using short-time Fourier transform and wavelet techniques, *Proc. Int. Conf. Maintenance and Reliability*, Vol. l, 2001, pp. 1401-1415.

[6] G. B. Kliman, Methods of motor current signature analysis, *Proc. Int. Conf. Power System*, Vol. 20, No. 5, 2000, pp. 463-174.

[7] W. Deleroi, Broken bars in squirrel cage rotor of an induction motor-Part 1: Description by superimposed fault currents, *Proc. Int. Conf. (in German) Arch. Elektrotech.*, Vol. 67, 2000, pp. 91-99.

[8] M. E. H. Benbouzid., Induction motor faults detection using advanced spectral analysis technique, *Proc. Int. Conf. Electrical Machines*, Vol. 3, Istanbul, Turkey, 1998, pp. 1849-1854.

[9] T. W.S. Chow, Three phase induction machines asymmetrical faults identification using bispectrum analysis, *IEEE Trans. Energy Conversion*, Vol. 10, 1995, pp. 688-693.